Silicene/germanene on MgX2 (X = Cl, Br, and I) for Li-ion battery applications

Zhu, J, Chroneos, A & Schwingenschlögl, U

Silicene/Germanene on MgX_2 (X = Cl, Br, and I) for Li-Ion Battery Applications

Jiajie Zhu[1], Alexander Chroneos[2,3,a] and Udo Schwingenschlögl[1,b]

[1]PSE Division, KAUST, Thuwal 23955-6900, Kingdom of Saudi Arabia

[2]Department of Materials, Imperial College, London SW7 2AZ, United Kingdom

[3]Faculty of Engineering and Computing, Coventry University, Priory Street,

Coventry CV1 5FB, United Kingdom

[a]Email: alexander.chroneos@imperial.ac.uk

[b]Email: udo.schwingenschlogl@kaust.edu.sa

September 30, 2015

Abstract

Silicene is a promising electrode material for Li-ion batteries due to a high Li capacity and low Li diffusion barrier. Germanene is expected to show a similar performance due to its analogous structural and electronic properties. However, the performance of both materials will be determined by the substrate, since freestanding configurations are instable. We propose MgX_2 (X = Cl, Br, and I) as suitable substrates, based on first-principles calculations. We find that Li will not cluster and that the Li capacity is very high (443 and 279 mAh/g for silicene and germanene on $MgCl_2$, respectively). Sandwich structures can be used to further enhance the performance. Low diffusion barriers of less than 0.3 eV are predicted for all the substrates.

1 Introduction

Li-ion batteries are key energy storage systems, which are applied, for example, in portable electronic devices, electric vehicles, and large scale power grids due to their high energy density and low maintenance costs.[1] Since the performance depends critically on the electrodes, various two-dimensional materials, including MXenes,[2] graphene,[3] and silicene[4] have been studied as possible replacements for the commercial graphite anode in order to make use of the high Li capacities resulting from large surface-to-volume ratios. For the MXenes a Li capacity of up to 410 mAh/g has been reported, exceeding that of graphite (372 mAh/g).[5] However, the stability and Li diffusion are strongly affected by the functional groups terminating the MXenes, which are very difficult to control.[6–8] Although pristine graphene provides a high Li capacity of 540 mAh/g,[9] the huge Li diffusion barrier inhibits application of the material.[10] Incorporation of double vacancies in the graphene lattice is predicted to strongly reduce the diffusion barrier to 1.34 eV, which, however, is still much higher than in graphite (0.22 eV).[10] Pristine silicene has an even higher Li capacity of 954 mAh/g and at the same time provides a low Li diffusion barrier of 0.23 eV.[11] Single and double vacancies enable diffusion through the sheet with the barries of 0.88 and 0.05 eV, respectively, as compared to the value of 1.59 eV in the pristine case.[12] In addition, by B substitution in silicene the Li capacity can be enhanced to 1410 mAh/g.[13]

Silicene has been successfully deposited on several metallic substrates including Ag(111),[14,15] Ir(111),[16] and ZrB_2(0001).[17] However, the interaction with the substrates destroys the linear dispersion of the π and π^* bands crossing the Fermi level at the K points of the Brillouin zone (Dirac cone).[18] As a consequence, also the promising Li capacity and Li diffusion barrier of the pristine material are lost. Various semiconducting substrates with much weaker interaction have been explored in the literature, including GaS, WSe_2, and MgX_2 (X = Cl, Br, and I): Although GaS preserves the Dirac cone of silicene, the large lattice mismatch of 7.5% is a major drawback.[19] WSe_2 would fit much better (lattice mismatch of 0.6%) but silicene on this substrate develops a large band gap of 0.3 eV.[20] MgX_2 (X = Cl, Br, and I), on the other hand, combines a reasonably small lattice mismatch with an almost gapless Dirac cone and a Fermi velocity comparable to freestanding silicene.[21] In addition, the small specific mass of the substrate is promising for achieving a high Li capacity. Battery-related properties of germanene have not been reported so far. The material recently has been deposited on Ag(111) and Pt(111) substrates, showing a similarly strong interaction as silicene.[22,23] In the present work we will demonstrate that silicene and germanene on semiconducting MgX_2 (X = Cl, Br, and

I) are suitable for Li battery applications, as the electronic properties of the freestanding materials are largely maintained.

2 Computational method

The calculations are carried out in the framework of density functional theory using the projector augmented wave method as implemented in Vienna Ab-initio Simulation Package.[24] The generalized gradient approximation in the flavor of Perdew, Burke and Ernzerhof for the exchange-correlation potential is employed together with the DFT-D3 van der Waals correction.[25] We use a $6 \times 6 \times 1$ mesh for the Brillouin zone integrations. The cut-off energy for the plane wave basis is set to 500 eV and the energy criterion for the self-consistency to 10^{-6} eV. All structures are relaxed until the residual forces on the atoms have declined to less than 0.01 eV/Å. We built $2 \times 2 \times 1$ supercells of silicene or germanene on top of MgX_2 (referred to as Si/MgX_2 and Ge/MgX_2) followed by a vacuum slab of 15 Å thickness to avoid artificial interaction because of the periodic boundary conditions. We have checked that the Li diffusion barriers calculated for a $3 \times 3 \times 1$ supercell deviate by less than 5% from the results reported in the following. Energy barriers and diffusion paths are calculated by the nudged elastic band method[26] with 7 to 9 images between the initial and final configurations.

3 Results and discussion

Since the weak van der Waals interaction between silicene/germanene and the substrates leads to large interlayer distances of more than 3.2 Å, Li atoms not only can be absorbed on the surface but also can be intercalated at the interface. Figure 1 illustrates the possible locations of the Li atoms: top, valley, and hollow sites on the surface (S-T, S-V, and S-H) and at the interface (I-T, I-V, and I-H). The S-T (I-T) site is located above (below) a Si atom in the upper sublattice of buckled silicene/germanene, the S-V (I-V) site above (below) a Si atom in the lower sublattice, and the S-H (I-H) site above (below) the center of a Si hexagon. Figure 1 demonstrates for the $Si/MgCl_2$ system the distortions of the silicene sheet induced by the interaction with Li, which can be quite substantial. For the other substrates as well as for the germanene systems similar distortions are observed.

Table 1 compares the total energies per atom obtained for the different structures. For the $MgCl_2$ and $MgBr_2$ substrates the six-coordinated hollow sites are energetically favorable over the four-coordinated top and valley sites. In addition intercalation is favorable over surface decoration.
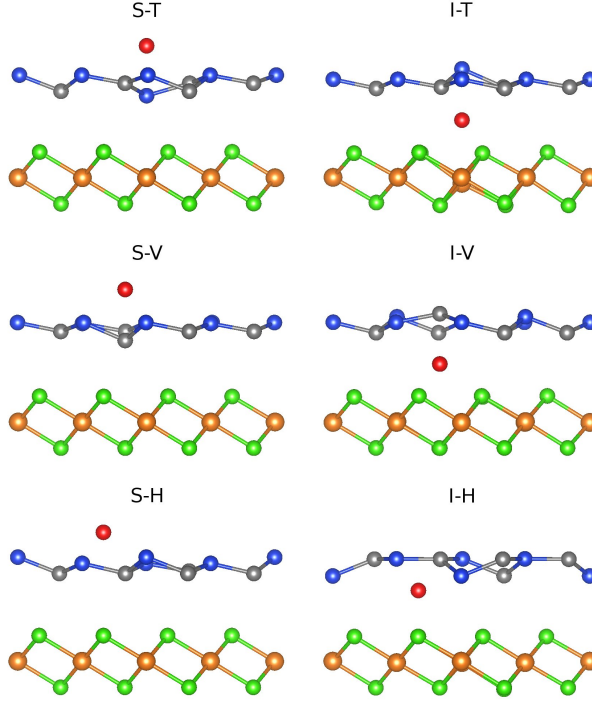
Figure 1: Structures of Li decorated Si/MgCl$_2$, see the text for details. The Mg, Cl, Si in upper sublattice and lower sublattice, and Li atoms are shown in brown, green, blue, gray, and red color.

Table 1: Total energies per atom, given with respect to the lowest energy structure.

	S-T (meV)	S-V (meV)	S-H (meV)	I-T (meV)	I-V (meV)	I-H (meV)
Si/MgCl$_2$	32	21	14	12	18	0
Ge/MgCl$_2$	23	17	8	8	8	0
Si/MgBr$_2$	28	16	8	5	8	0
Ge/MgBr$_2$	27	14	5	2	5	0
Si/MgI$_2$	—	16	7	0	—	5
Ge/MgI$_2$	—	16	4	0	—	2

For the MgI$_2$ substrate the S-T and I-V configurations are instable and converge to the S-V and I-T configurations, respectively. Intercalation at the top site here is favorable for both silicene and germanene. In general, the energy differences between the structures are small, often going close to degeneracy. The energetics of the Li decoration can be described by the formation energy

$$\Delta H = E_{\text{decorated}} - E_{\text{nondecorated}} - E_{\text{Li}}, \tag{1}$$

given by the total energies of the decorated and nondecorated systems as well as the total energy of a Li atom in bulk Li. Negative values between -1.29 eV and -0.62 eV are obtained increasing from MgCl$_2$ to MgI$_2$, showing that Li does not form clusters.

A large Li capacity is important to achieve a high energy density in Li-ion batteries. The maximal number of Li atoms that can be accommodated without breaking the silicene/germanene sheet is found to be 10 for MgCl$_2$ and MgBr$_2$ (6 located on the surface and 4 at the interface) and 9 for MgI$_2$

Table 2: Comparison of the calculated Li capacities.

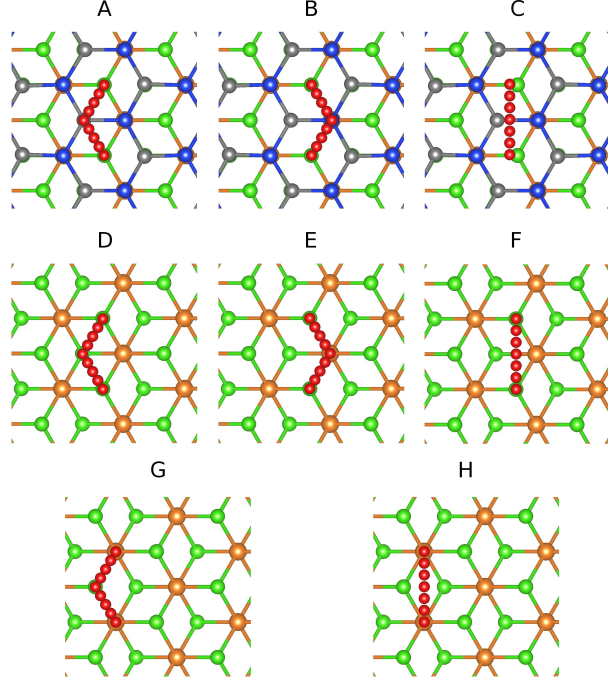|	MgCl$_2$ (mAh/g)	MgBr$_2$ (mAh/g)	MgI$_2$ (mAh/g)
Si/MgX$_2$	443	279	180
Si/MgX$_2$/Si	646	452	309
Ge/MgX$_2$	279	203	142
Ge/MgX$_2$/Ge	347	282	212

Figure 2: Li diffusion paths on the surface (A-C) and at the interface (D-H) of the Si/MgX$_2$ and Ge/MgX$_2$ (X = Cl, Br and I) systems, see the text for details.

(5 located on the surface and 4 at the interface), in the $2 \times 2 \times 1$ supercell. This corresponds to 2.5 and 2.25 Li atoms per silicene/germanene unit cell, which exceeds the value of 2 for freestanding silicene (in agreement with Ref. 11) and germanene. We observe that Si/MgX$_2$/Si and Ge/MgX$_2$/Ge sandwich structures can accommodate twice the number of Li atoms, since the separation between the two silicene/germanene sheets is more than 9 Å. The Li capacity[27] of freestanding germanene (369 mAh/g) is much smaller than that of freestanding silicene (954 mAh/g), which is in excellent agreement with other theoretical value,[11] due to the higher mass of Ge as compared to Si. Table 2 lists the Li capacities for the systems under investigation. The values decrease from MgCl$_2$ to MgI$_2$ because of the growing mass of the substrate. We find that the Si/MgCl$_2$ and Si/MgCl$_2$/Si systems achieve 46% and 68% of the Li capacity of freestanding silicene, respectively, and thus clearly outperform graphite and the MXenes.[5,11] The Li capacity of the Ge/MgCl$_2$/Ge system is comparable to that of freestanding germanene.

The cycling rate depends on the Li diffusion barrier. The diffusion barrier for freestanding silicene is calculated to be 0.20 eV, which is in good agreement with the reported value of 0.23 eV.[11] The
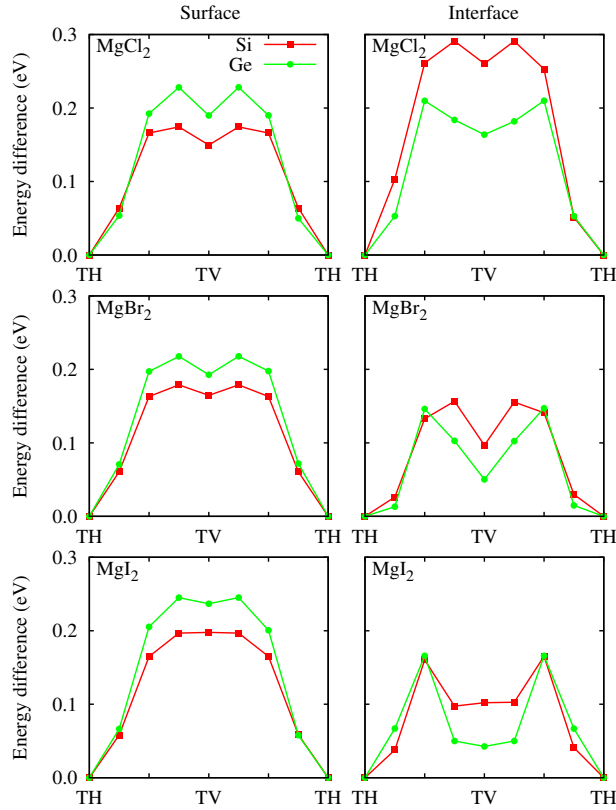
Figure 3: Li diffusion barriers on the surface and at the interface for the Si/MgX$_2$ and Ge/MgX$_2$ (X = Cl, Br and I) systems.

Table 3: Li diffusion barriers on the surface and at the interface for the Si/MgX$_2$ and Ge/MgX$_2$ (X = Cl, Br and I) systems.

	MgCl$_2$ (eV)	MgBr$_2$ (eV)	MgI$_2$ (eV)
	Surface		
Silicene	0.17	0.18	0.20
Germanene	0.23	0.22	0.25
	Interface		
Silicene	0.29	0.16	0.16
Germanene	0.21	0.15	0.16

corresponding value of freestanding germanene turns out to be 0.29 eV. We consider the three surfaces diffusion paths (A, B, and C) from hollow site to hollow site shown in Figure 2. Paths A and B (9 images) pass the valley and top sites, respectively, whereas path C (7 images) directly connects the initial and final states. Path C always converges to path A, which turns out to be the minimum energy path for all systems. For path A the energies are illustrated in Figure 3 and the diffusion barriers are summarized in Table 3. The calculated values are substantially smaller than for freestanding silicene and germanene, reflecting a homogeneous surface charge distribution. In general the silicene systems are favorable over the germanene systems. The transition state is always located close to the valley site, which forms a local energy minimum. The energy difference between the transition state and this minimum decreases from MgCl$_2$ to MgI$_2$.

Similar paths (D, E and F) are considered for interface diffusion in the cases of the MgCl$_2$ and MgBr$_2$ substrates (Figure 3), whereas the initial and final states are set to the top site for the MgI$_2$ substrate (paths H and G). The corresponding minimum energy paths turn out to be paths E and H. The calculated diffusion barrier for the Si/MgCl$_2$ system is only slightly larger than for freestanding silicene, see Table 3. All other systems exhibit smaller values than freestanding silicene/germanene. In general, silicene results in larger interface diffusion barriers than germanene. Interestingly, for the Si/MgCl$_2$ system diffusion is easier at the interface than on the surface. The transition state of the interface diffusion is located between the hollow and top sites and there appears a local energy minimum at the top site for the MgCl$_2$ and MgBr$_2$ subtrates. Li diffusion through the silicene/germanene sheets is almost impossible due to a high diffusion barrier of 1.47/0.95 eV, which is similar to the theoretical value of 1.59 eV for freestanding silicene.[12] Although vacancies can reduce this barrier, their concentration is typically low. Therefore, the Li atoms will diffuse mainly on the surface and at the interface.

4 Conclusions

Our first-principles calculations demonstrate that silicene/germanene attached to MgX$_2$ (X = Cl, Br and I) gives rise to interesting hybrid materials for Li-ion battery applications. Li atoms are not incline to form clusters on the surface and at the interface in each case. The presence of the substrates enhances the number of Li atoms that can be stored by one unit cell of silicene/germanene. On MgCl$_2$ the Li capacity of the hybrid systems reaches 68% and 94% of the values previously reported for freestanding silicene and germanene, respectively. MgBr$_2$ and MgI$_2$ suffer from their larger masses. As compared to freestanding silicene/germanene we obtain for MgCl$_2$ lower or at least comparable Li diffusion barriers on the surface as well as at the interface. Therefore, Si/MgCl$_2$ and Ge/MgCl$_2$ are promising hybrid materials for the electrodes of Li-ion batteries, since the excellent performance of the pristine Dirac materials silicene and germanene is preserved and even enhanced.

Acknowledgement

References

[1] Dunn, B.; Kamath, H.; Tarascon, J.-M. Electrical Energy Storage for the Grid: A Battery of Choices. *Science* **2011**, *334*, 928–935.

[2] Naguib, M.; Mochalin, V. N.; Barsoum, M. W.; Gogotsi, Y. 25th Anniversary Article: MXenes: A New Family of Two-Dimensional Materials. *Adv. Mater.* **2014**, *26*, 992–1005.

[3] Novoselov, K. S.; Geim, A. K.; Morozov, S. V.; Jiang, D.; Zhang, Y.; Dubonos, S. V.; Grigorieva, I. V.; Firsov, A. A. Electric Field Effect in Atomically Thin Carbon Films. *Science* **2004**, *306*, 666–669.

[4] Cahangirov, S.; Topsakal, M.; Aktürk, E.; Şahin, H.; Ciraci, S. Two- and One-Dimensional Honeycomb Structures of Silicon and Germanium. *Phys. Rev. Lett.* **2009**, *102*, 236804.

[5] Mashtalir, O.; Naguib, M.; Mochalin, V. N.; DallAgnese, Y.; Heon, M.; Barsoum, M. W.; Gogotsi, Y. Intercalation and Delamination of Layered Carbides and Carbonitrides. *Nat. Commun.* **2013**, *4*, 1716.

[6] Tang, Q.; Zhou, Z.; Shen, P. Are MXenes Promising Anode Materials for Li Ion Batteries? Computational Studies on Electronic Properties and Li Storage Capability of Ti_3C_2 and $Ti_3C_2X_2$ (X = F, OH) Monolayer. *J. Am. Chem. Soc.* **2012**, *134*, 16909–16916.

[7] Xie, Y.; DallAgnese, Y.; Naguib, M.; Gogotsi, Y.; Barsoum, M. W.; Zhuang, H. L.; Kent, P. R. C. Prediction and Characterization of MXene Nanosheet Anodes for Non-Lithium-Ion Batteries. *ACS Nano* **2014**, *8*, 9606–9615.

[8] Li, Z.; Wang, L.; Sun, D.; Zhang, Y.; Liu, B.; Hu, Q.; Zhou, A. Synthesis and Thermal Stability of Two-Dimensional Carbide MXene Ti_3C_2. *Mater. Sci. Eng. B* **2015**, *191*, 33–40.

[9] Yoo, E.; Kim, J.; Hosono, E.; Zhou, H.-S.; Kudo, T.; Honma, I. Large Reversible Li Storage of Graphene Nanosheet Families for Use in Rechargeable Lithium Ion Batteries. *Nano Lett.* **2008**, *8*, 2277–2282.

[10] Das, D.; Kim, S.; Lee, K.-R.; Singh, A. K. Li Diffusion through Doped and Defected Graphene. *Phys. Chem. Chem. Phys.* **2013**, *15*, 15128–15134.

[11] Tritsaris, G. A.; Kaxiras, E.; Meng, S.; Wang, E. Adsorption and Diffusion of Lithium on Layered Silicon for Li-Ion Storage. *Nano Lett.* **2013**, *13*, 2258–2263.

[12] Setiadi, J.; Arnold, M. D.; Ford, M. J. Li-Ion Adsorption and Diffusion on Two-Dimensional Silicon with Defects: A First Principles Study. *ACS Appl. Mater. Interface* **2013**, *5*, 10690–10695.

[13] Tan, X.; Cabrera, C. R.; Chen, Z. Metallic BSi_3 Silicene: A Promising High Capacity Anode Material for Lithium-Ion Batteries. *J. Phys. Chem. C* **2014**, *118*, 25836–25843.

[14] Vogt, P.; De Padova, P.; Quaresima, C.; Avila, J.; Frantzeskakis, E.; Asensio, M. C.; Resta, A.; Ealet, B.; Le Lay, G. Silicene: Compelling Experimental Evidence for Graphenelike Two-Dimensional Silicon. *Phys. Rev. Lett.* **2012**, *108*, 155501.

[15] Tsoutsou, D.; Xenogiannopoulou, E.; Golias, E.; Tsipas, P.; Dimoulas, A. Evidence for Hybrid Surface Metallic Band in (4×4) Silicene on Ag(111). *Appl. Phys. Lett.* **2013**, *103*, 231604.

[16] Meng, L.; Wang, Y.; Zhang, L.; Du, S.; Wu, R.; Li, L.; Zhang, Y.; Li, G.; Zhou, H.; Hofer, W. A.; Gao, H. Buckled Silicene Formation on Ir(111). *Nano Lett.* **2013**, *13*, 685–690.

[17] Fleurence, A.; Friedlein, R.; Ozaki, T.; Kawai, H.; Wang, Y.; Yamada-Takamura, Y. Experimental Evidence for Epitaxial Silicene on Diboride Thin Films. *Phys. Rev. Lett.* **2012**, *108*, 245501.

[18] Wang, Y.; Cheng, H. Absence of a Dirac Cone in Silicene on Ag(111): First-Principles Density Functional Calculations with a Modified Effective Band Structure Technique. *Phys. Rev. B* **2013**, *87*, 245430.

[19] Ding, Y.; Wang, Y. Electronic Structures of Silicene/GaS Heterosheets. *Appl. Phys. Lett.* **2013**, *103*, 043114.

[20] Zhu, J.; Schwingenschlögl, U. Stability and Electronic Properties of Silicene on WSe$_2$. *J. Mater. Chem. C* **2015**, *3*, 3946–3953.

[21] Zhu, J.; Schwingenschlögl, U. Structural and Electronic Properties of Silicene on MgX$_2$ (X = Cl, Br, and I). *ACS Appl. Mater. Interface* **2014**, *6*, 11675–11681.

[22] Golias, E.; Xenogiannopoulou, E.; Tsoutsou, D.; Tsipas, P.; Giamini, S. A.; Dimoulas, A. Surface Electronic Bands of Submonolayer Ge on Ag(111). *Phys. Rev. B* **2013**, *88*, 075403.

[23] Li, L.; Lu, S.-Z.; Pan, J.; Qin, Z.; Wang, Y.-Q.; Wang, Y.; Cao, G.-Y.; Du, S.; Gao, H.-J. Buckled Germanene Formation on Pt(111). *Adv. Mater.* **2014**, *26*, 4820–4824.

[24] Kresse, G.; Joubert, D. From Ultrasoft Pseudopotentials to the Projector Augmented-Wave Method. *Phys. Rev. B* **1999**, *59*, 1758–1775.

[25] Grimme, S.; Antony, J.; Ehrlich, S.; Krieg, H. A Consistent and Accurate Ab Initio Parametrization of Density Functional Dispersion Correction (DFT-D) for the 94 Elements H-Pu. *J. Chem. Phys.* **2010**, *132*, 154104.

[26] Mills, G.; Jónsson, H.; Schenter, G. K. Reversible Work Transition State Theory: Application to Dissociative Adsorption of Hydrogen. *Surf. Sci.* **1995**, *324*, 305–337.

[27] Er, D.; Li, J.; Naguib, M.; Gogotsi, Y.; Shenoy, V. B. Ti$_3$C$_2$ MXene as a High Capacity Electrode Material for Metal (Li, Na, K, Ca) Ion Batteries. *ACS Appl. Mater. Interface* **2014**, *6*, 11173–11179.